Characterization and Application of Nanomaterials 2024, 7(1), 3587.
https://doi.org/10.24294/can.v7i1.3587

Article

Mo-doped titanate nanofibers from hydrothermal syntheses for improving bone scaffold

Yang Tian[1,2,†], Lu Zhang[3,†], Yiting Xiao[4,†], Trenton Collins[5], Abdussamad Akhter[5], Yan Huang[6], Z. Ryan Tian[1,2,3,5,*]

[1] Department of Materials Science and Engineering, University of Arkansas, Fayetteville, AR 72701, USA.
[2] Institute for Nanoscience and Engineering, University of Arkansas, Fayetteville, AR 72701, USA.
[3] Department of Cell and Molecular Biology, University of Arkansas, Fayetteville, AR 72701, USA.
[4] Department of Biological and Agricultural Engineering, University of Arkansas, Fayetteville, AR 72701, USA.
[5] Department of Chemistry and Biochemistry, University of Arkansas, Fayetteville, AR 72701, USA.
[6] Department of Animal Science, University of Arkansas, Fayetteville, AR 72701, USA.
*** Corresponding author:** Z. Ryan Tian, rtian@uark.edu
[†] *These authors contributed equally to this work.*

CITATION

Tian Y, Zhang L, Xiao Y, et al. Mo-doped titanate nanofibers from hydrothermal syntheses for improving bone scaffold. Characterization and Application of Nanomaterials. 2024; 7(1): 3587. https://doi.org/10.24294/can.v7i1.3587

ARTICLE INFO

Received: 9 December 2023
Accepted: 9 January 2024
Available online: 18 January 2024

Abstract: A longstanding interest in bone tissue engineering is the development of new bio-scaffolds that can be manufactured on a large scale with high throughput at low cost. Here, we report a low-cost and systematically optimized hydrothermal synthesis for producing Mo-doped potassium titanate nanofibers with high structural purity. This new nanosynthesis is based on bone tissue growth on an undoped titanate nanowires-entangled scaffold, as previously reported by our team. The morphological and structural characterization data suggest that the crystal structure of Mo-doped titanate nanofibers closely resembles that of the undoped ones. This resemblance is potentially valuable for assessing the role of Mo dopants in engineering bone tissue.

Keywords: nanosynthesis; titanate nanofiber; bone scaffold; molybdenum dopant

1. Introduction

Exploiting new methods for synthesizing biocompatible nanowires with novel structures and surface properties is critical to the development of new tissue engineering scaffolds. The nanowires-entangled scaffolds with well-tuned surface chemistry (e.g., the surface energy, protein adsorption, and pore structure) can facilitate a programmable release of growth hormones, drugs, and nutrients to promote the osteoblast cells adhesion, proliferation, and differentiation, thus-upgrading the bio-scaffolds versatilities [1]. Further, doping valve metal atoms in the nanowire structure or on the nanowire surface can enhance the scaffold's radio-opacity to boost the orthopedic X-ray imaging's contrast, i.e., resolution [2–6]. Under these inspirations, this work has successfully doped and optimized the nanowire analogs of natural bone scaffold, in a series of systematic syntheses for doping the scaffold nanowire rationally using different valve metals in different doping ratios. Thus, varied properties of the nanowires, such as aspect ratio, surface chemistry, and the chemical environment of the doping atoms, are anticipated to provide new insights into the role of valve metals in bone implants [1].

Titanium dioxide (TiO2) has been attracting enormous interest in both nanomaterial chemistry and orthopedic nanomedicine. The TiO_2-based nanosyntheses have typically resulted in a clay-like layered titanate structure in the nanowire [7] or

nanotube [8] morphologies, with the edge-sharing [TiO_6] octahedra in the negatively charged layer and the cations intercalating in between the layers, which can promote the hydroxyapatite nucleation and formation on the nanowire surface quickly in a simulated body fluid (SBF) [9]. In a hydrothermal treatment, the TiO_2 powders (regardless of the rutile or anatase phase) originally suspended in an aqueous KOH solution can quickly start to form the K-titanate of one-dimensional (1D) nanowires [10]. The resultant layered 1D-nanostructure can act like a cation "reservoir", facilitating the ion-exchange of K^+ with other cations in the body fluids. This allows for an autonomous, real-time balance of cations *in situ*, on which the bone tissue growth can be promoted. Here, the K-titanate, in a hypotonic condition with respect to the plenty of calcium (Ca^{2+}) ions nearby, can prompt the ion-exchange of K^+ ions with the Ca^{2+} in SBF. Subsequently, the phosphate anions in the body fluid, including $(PO_4)^{3-}$, $(HPO_4)^{2-}$, and $(H_2PO^4)^-$, can support the interactions with the Ca^{2+} ions on the titanate surface. This interaction results in the formation of hydrated calcium phosphate, commonly referred to as hydroxyapatite, which is a vital component of natural bone and essential for establishing an osteogenic/osteoconductive environment [9].

In addition, nanomaterials containing valve metals such as Molybdenum (Mo), Zirconium (Zr), Niobium (Nb), or Tantalum (Ta) can help improve the osteointegration [10–16]. Here, the Mo ions can promote the immunomodulation and facilitate bone repair by comodulating the balance between bone formation and resorption, showing a good potential to help regenerate bones [12]. Further, the Mo-based nanomaterials syntheses in literature should be optimized to meet the need for large-scale productions. Moreover, doping the relatively expensive valve metals on or in the low-cost titanate scaffold nanowire can reduce the cost and the valve metals cytotoxicity to the bone tissue. In this work, we systematically conducted nanosynthesis to produce long and pristine Mo-doped titanate nanofibers with the good feasibility for mass-production of the new orthopedic implants. The doping ratio was optimized using the structural, morphological, and chemical characterizations data from the scanning electron microscopy with an energy-dispersive elemental analyzer (SEM-EDX), X-ray diffraction (XRD), and X-ray photoelectron spectroscopy (XPS).

2. Materials and methods

2.1. Nanowire synthesis

The Mo-doped potassium titanate nanowires were prepared following a protocol in literature [10,17–20] with some modifications. Briefly, in a Teflon cup containing 50 mL water solution of 10M KOH, 500 mg of TiO_2 powder (Aeroxide P25) was added in and stirred for about 5 min with a Teflon-coated magnetic stirring bar on an electrical stirrer. Thereafter, Molybdenum oxide powder (from Alfa Aesar) was mixed into the Teflon cup to form a mixture upon stirring. Here, the weight ratio of Mo-dopant to titanate was in the range of 1%–4%.

Next, the mixture containing Teflon cup was sealed in an autoclave container, heated in an oven at 240 ℃ for 72 h and then cooled down in air. The white powdery product was collected, water-washed to pH = 7, and oven-dried at 60 ℃ for the

characterizations. To keep the nanowire lattice intact, it is important to do the water-washing step carefully, as detailed separately below.

2.2. Characterizations

The SEM-EDX analysis was done on the FEI Nova NanoLab 200 to check the nanowires morphology and chemical composition. Typically, a nanowire sample was placed on an aluminum holder to let the sample dry in air, then surface-coated with Au in a plasma sputtering coater. The XRD analysis was performed on the Rigaku MiniFlex II Desktop X-ray diffractometer using monochromatized Cu-Kα ($\lambda = 1.5406$ Å) at 30 kV and 15 mA, in the range of 2θ from 5° to 60° at a speed of 1°/min. The XPS characterization was conducted on the PHI VersaProbe Scanning XPS system to study the chemical environment of Mo.

3. Results and discussions

3.1. Evidence of the novel Mo-doping

The Mo-doped potassium titanate nanowires underwent a self-assembly process, resulting in the formation of a bio-scaffold, as illustrated in **Figure 1**. This self-assembled nanofibrous scaffold has pores in the size of tens of microns (**Figure 1(a)**) to support the effective adhesion of osteoblast cells into the pores, while the pore wall (of self-entangled nanowires) is also highly porous (**Figure 1(b)**) to allow the osteoblast cells' nutrients and metabolites to diffuse quickly across.

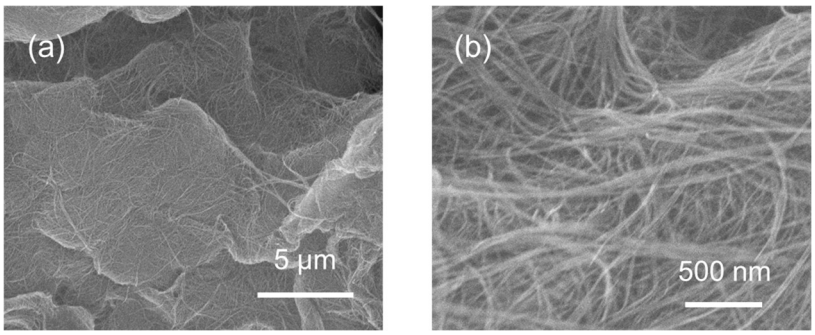

Figure 1. SEM micrographs of Mo-doped potassium titanate.

Upon examination at a higher magnification (**Figure 2(a)**), the clean and well-crystallized long nanowires in self-entangled form can be clearly seen, which is a characteristic of the Mo-doped potassium titanate nanowires. The nanofibers length extends into tens of microns, while retaining their width below 100 nm. In addition, **Figure 2(a)** shows the relatively smooth surface of the high length-to-width ratio (or aspect ratio) nanofibers, suggesting the optimal control over the nanowires' nucleation and 1D-growth in nanoscale, which is crucial for the Mo-dopant's good distribution throughout the crystal lattice of all the nanowires from the "one-pot" nanosynthesis.

In the Energy-Dispersive X-ray (EDX) spectroscopy mapping (**Figure 2(b)**), the Mo dopants exhibit a uniform distribution in the nanofibers. This uniformity in distribution suggests the dopant well-dispersed in the Mo-doped potassium titanate nanowires, which is indicative of a quite precisely controlled nano-synthesis process. In theory, the [MoO_6] octahedron in the nanowire lattice is larger than the [TiO_6]

octahedra [21]. However, this size difference-induced structural distortions were well-tolerated without compromising the overall lattice continuity, as suggested by the EDX mapping in **Figure 2**. Intuitively, the good dispersion of Mo allows each [MoO_6] octahedron to integrate into the lattice without disrupting the structural integrity, thus keeping the framework intact everywhere. In other words, the high dispersion of Mo dopant in the nanofiber structure suggests the optimal doping conditions that support the **Figure 1**.

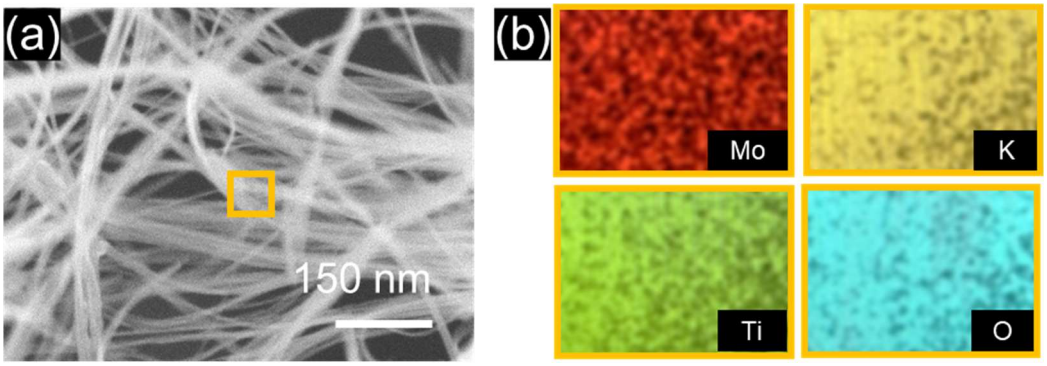

Figure 2. The EDX Mapping of the Mo-doped Potassium Titanate Nanofibers. **(a)** The high-resolution SEM of Mo-doped potassium with the yellow box for EDX mapping. **(b)** The EDX mapping showed that the Mo, K, Ti, and O are evenly distributed on the titanate nanowires.

The nanofiber crystal structure was further characterized using the XRD patterns (**Figure 3**). All the XRD peaks of (200), (110), (310), (31$\bar{2}$), (40$\bar{4}$), and (020) can be assigned to the layered $K_2Ti_6O_{13}$ titanate lattice (JCPDS No. 40-0403). The XRD patterns of titanate nanofibers with various doping ratios were identical and no residual impurity was detected, as evidenced by no extra peaks in the XRD pattern with respect to the XRD detection limit, which again indicates that the larger [MoO_6] octahedron was evenly doped in the titanate crystal structure to maintain the lattice integrity and nanowire structure.

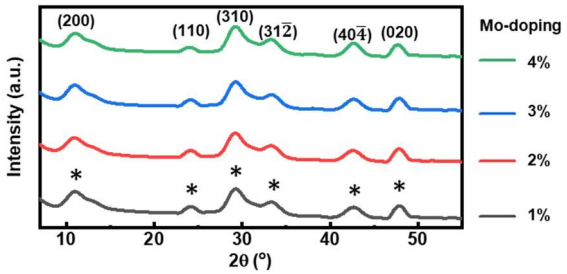

Figure 3. X-Ray diffraction of Mo-doped potassium titanate nanofibers with doping percentage.

Comparing the XRD patterns with and without the Mo-dopants (**Figure 4(a)**), the large Mo-dopant increases the d-space between adjacent titanate sheets by shifting the XRD peak to $d_{(200)}$ = 8.0919 Å (or a lower 2-theta angle at 2θ = 11.03°). This is in contrast with the undoped nanowire's smaller d-space of $d_{(200)}$ = 7.7415 Å at a higher 2-theta angle (2θ = 11.43°). This interlayer spacing expansion is indicative of Mo substitutional doping within the titanate lattice. More specifically, the ionic radius of Mo^{5+} (75 pm) and Mo^{6+} (73 pm) is larger than that of Ti^{4+} (53 pm) which leads to interlayer spacing expansion with $Mo^{5+/6+}$ replacing Ti^{4+} while without destroying the original lattice structure [21]. Equivalently, the Mo dopant's higher content can shift

the $d_{(200)}$ peak to a lower diffraction angle. The same shift happened to (110), (310), $(31\bar{2})$, and (020), as shown in **Figure A1**. Moreover, the doped samples XRD patterns show no structural impurity. Apparently, all the XRD peaks are in the same width and can be indexed to that of potassium titanate, matching what our lab reported in literature before [10,17,18].

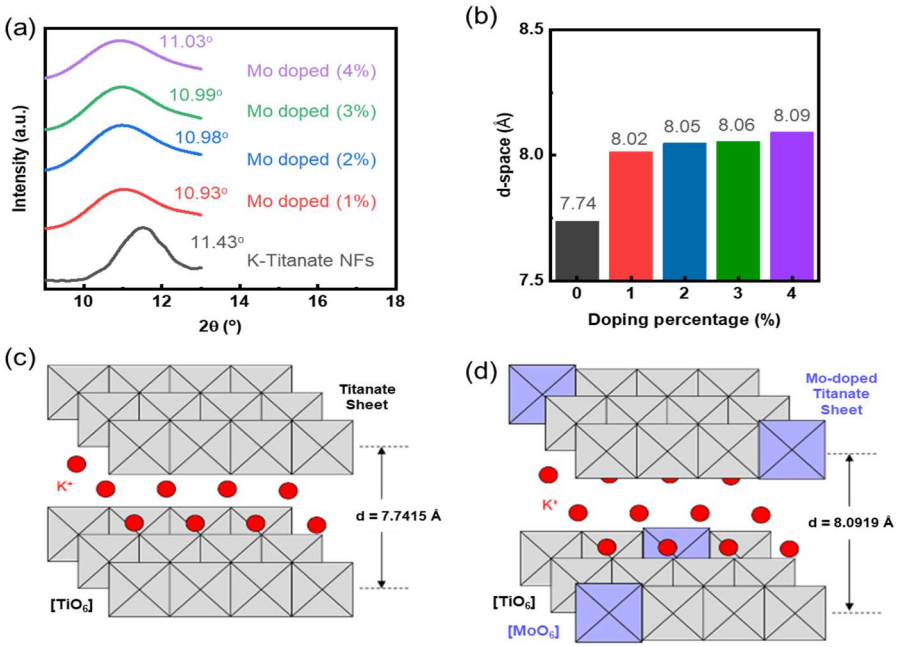

Figure 4. (a) XRD analysis of Mo-doped potassium titanate nanowires with **(b)** d-space. **(c)** and **(d)** the schematics for illustrating the Mo-dopant impact on the titanate crystal structure.

The XPS characterization investigated the chemical environment of the Mo dopant. The Mo $3d_{3/2}$ and $3d_{5/2}$ peaks of the 4% Mo-doped K-titanate nanofibers are presented in **Figure 5**. The peaks observed at 232.5 and 235.7 eV came from the Mo $3d_{5/2}$ and Mo $3d_{3/2}$ of Mo^{6+}, while the peaks at 231.9 and 235.0 eV came from the Mo $3d_{5/2}$ and Mo $3d_{3/2}$ of Mo^{5+} [22]. These characteristic peaks are attributed to Mo-O bonds, indicating the successful integration of Mo into the K-titanate lattice. Obtaining from the ratio of peak area, the atomic percentage of Mo^{6+} is 67.5% while that of Mo^{5+} is 32.5%, showing that Mo^{6+} is the main dopant form in the K-titanate nanofiber crystal lattice.

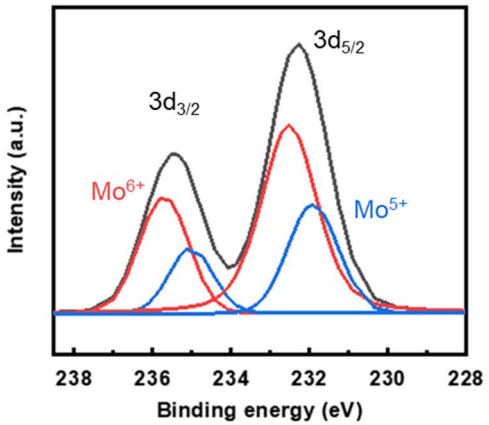

Figure 5. XPS spectroscopy of 4% Mo-doped potassium titanate nanofibers.

3.2. Lessons from the Mo-doping

Evidently, within the K-titanate nanofiber's clay-like layered crystal structure, the Ti^{4+}-based [TiO_6] octahedra were partially substituted by the Mo-based [MoO_6] octahedra, confirming the sterically challenging doping of Mo. Naturally, the larger [MoO_6] compared to [TiO_6] would position itself more easily on the nanofiber surface to reduce perturbations in the [TiO_6]-dominated nanowire crystal lattice. Such surface-exposed [MoO_6] units can be recognized by the osteoblast cell surface to facilitate the bone-tissue adhesion, as supported by the previous studies [12,13]. In this logic, the interlayer K^+ cations near the [MoO_6] could be rapidly substituted by the nearby Ca^{2+} cations in the body fluids. The Ca^{2+} cations' rapid exchange can in turn accelerate the formation of hydrated calcium phosphates, or hydroxyapatite, on the nanowire surface, matching the findings from other research groups using SBF [9,23], which supports this project's logic in the rational design. On this basis, the hydroxyapatite layer on the underlying titanate nanofiber should in turn support the sustained bone tissue adhesion on the hydroxyapatite-supported nanofiber, crafting an optimal osteogenic/osteo- conductive milieu [9], which is under an ongoing verification using the slow and tedious *in vitro* cell-culture experiments. The doping-modified titanate nanofibers surface characteristics has demonstrated a simple approach to existing methodologies in literature, for potentially improving the osteoconductivity of bone-scaffolds [10,12,15,18,24]. Fundamentally, this work found a new and manufacturing-viable route to incorporating Mo into the titanate nanowire matrix, which could be generally applicable to other subfields of the orthopedic nanomedicine.

4. Conclusions

Potassium titanate nanofibers doped with Mo have been successfully fabricated through a simple hydrothermal process, which to the best of our knowledge is quite new, especially in orthopedic nanomedicine. The doping process has been well-controlled to keep the nanowire's morphology, structure, and chemical composition intact. These are indicative of the successful development of an efficient and well-controlled doping method for varying the Mo dopant concentrations while preserving the nanowires lattice. This is critical for further optimizing the nanowires other properties for different applications. To evaluate the influence of this material in the field of bone tissue engineering, nanofibers with different concentrations of Mo-dopant have been investigating *in vitro* to determine their biocompatibility and osteogenic capabilities.

Currently, a critical and logical phase of the follow-up research is in progress, concentrating on the analysis of these nanofibers with systematically varied concentrations of Mo dopants, for specifically assessing these new nanowires biocompatibility and osteogenic potential. The investigation into the interactions between these Mo-doped nanofibers and bone cells is pivotal for acquiring a deeper understanding of their suitability as potential materials for bone implants. The thorough evaluation of the biocompatibility is pivotal to determining these materials viability in for medical applications, especially in the bone tissue regeneration. A forward-thinking strategy to expand upon this research entails the doping of titanate nanowires with, for example, dual oxide dopants. Such a new methodology could pave

the way for exploring a broader spectrum of bone implants of new types with the potentially greater physiological adaptability. Comprehending the biocompatible transition metals' doping impact on the physical and chemical properties of these nanowire-based bone implants is crucial and fruitful. This understanding is pivotal for the tailored customization of biomaterials to suit each unique application, ensuring their optimal performance and compatibility.

Finally, developing a diverse and novel family of doped titanate nanofibers, each characterized by distinct compositions and properties, constitutes a strategic approach for enabling researchers to systematically explore how variations in doping influence the material's characteristics and performance. Gathering such data is imperative for the precise optimization of these materials, tailoring them for specific uses in bone tissue engineering or other relevant fields.

Author contributions: Investigation, YT, YX, TC, and AA; writing—original draft preparation, YT, LZ, ZRT; writing—review and editing, YT, LZ, YH, and ZRT. All authors have read and agreed to the published version of the manuscript.

Funding: This work was partially supported from the NSF (Grant #2230853) and NIST (Grant #70NANB22H010).

Conflict of interest: The authors declare no conflict of interest. The funders had no role in the design of the study; in the collection, analyses, or interpretation of data; in the writing of the manuscript, or in the decision to publish the results.

Data availability statement: Applicable for reasonable request.

References

1. Gao C, Wei D, Yang H, et al. Nanotechnology for treating osteoporotic vertebral fractures. International Journal of Nanomedicine. 2015; 10: 5139–5157. doi: 10.2147/IJN.S85037
2. Zhang B, Li J, He L, et al. Bio-surface coated titanium scaffolds with cancellous bone-like biomimetic structure for enhanced bone tissue regeneration. Acta Biomaterialia. 2020; 114: 431–448. doi: 10.1016/j.actbio.2020.07.024
3. Min Q, Liu J, Zhang Y, et al. Dual network hydrogels incorporated with bone morphogenic protein-7-loaded hyaluronic acid complex nanoparticles for inducing chondrogenic differentiation of synovium-derived mesenchymal stem cells. Pharmaceutics. 2020; 12(7): 613. doi: 10.3390/pharmaceutics12070613
4. Wu T, Li B, Wang W, et al. Strontium-substituted hydroxyapatite grown on graphene oxide nanosheet-reinforced chitosan scaffold to promote bone regeneration. Biomaterials Science. 2020; 8(16): 4603–4615. doi: 10.1039/D0BM00523A
5. Oudadesse H, Najem S, Mosbahi S, et al. Development of hybrid scaffold: Bioactive glass nanoparticles/chitosan for tissue engineering applications. Journal of Biomedical Materials Research Part A. 2021; 109(5): 590–599. doi: 10.1002/jbm.a.37043
6. Nie L, Deng Y, Li P, et al. Hydroxyethyl chitosan-reinforced polyvinyl alcohol/biphasic calcium phosphate hydrogels for bone regeneration. ACS Omega. 2020; 5(19): 10948–10957. doi: 10.1021/acsomega.0c00727
7. Aldaadaa A, Qaysi M, Knowles J. Physical properties and biocompatibility effects of doping SiO_2 and TiO_2 into phosphate-based glass for bone tissue engineering. Journal of Biomaterials Applications. 2018; 33(2): 271–280. doi: 10.1177/08853282187888
8. Hashemi A, Ezati M, Mohammadnejad J, et al. Chitosan coating of TiO_2 nanotube arrays for improved metformin release and osteoblast differentiation. International Journal of Nanomedicine. 2020; 15: 4471–4481. doi: 10.2147/IJN.S248927
9. Liang F, Zhou L, Wang K. Apatite formation on porous titanium by alkali and heat-treatment. Surface and Coatings Technology. 2003; 165(2): 133–139. doi: 10.1016/S0257-8972(02)00735-1
10. Cole P, Tian Y, Thornburgh S, et al. Hydrothermal synthesis of valve metal Zr-doped titanate nanofibers for bone tissue engineering. Nano and Medical Materials. 2023; 3(2): 249. doi: 10.59400/nmm.v3i2.249

11. Awasthi GP, Kaliannagounder VK, Maharjan B, et al. Albumin-induced exfoliation of molybdenum disulfide nanosheets incorporated polycaprolactone/zein composite nanofibers for bone tissue regeneration. Materials Science and Engineering: C. 2020; 116: 111162. doi: 10.1016/j.msec.2020.111162
12. Tian B, Li X, Zhang J, et al. A 3D-printed molybdenum-containing scaffold exerts dual pro-osteogenic and anti-osteoclastogenic effects to facilitate alveolar bone repair. International Journal of Oral Science. 2022; 14(1): 1–18. doi: 10.1038/s41368-022-00195-z
13. Vasto S, Baldassano D, Sabatino L, et al. The role of consumption of molybdenum biofortified crops in bone homeostasis and healthy aging. Nutrients. 2023; 15(4): 1022. doi: 10.3390/nu15041022
14. Wu S, Wang J, Jin L, et al. Effects of polyacrylonitrile/MoS_2 composite nanofibers on the growth behavior of bone marrow mesenchymal stem cells. ACS Applied Nano Materials. 2018; 1(1): 337–343. doi: 10.1021/acsanm.7b00188
15. Marins NH, Lee BEJ, e Silva RM, et al. Niobium pentoxide and hydroxyapatite particle loaded electrospun polycaprolactone/gelatin membranes for bone tissue engineering. Colloids and Surfaces B: Biointerfaces. 2019; 182: 110386. doi: 10.1016/j.colsurfb.2019.110386
16. Frandsen CJ, Brammer KS, Noh K, et al. Tantalum coating on TiO_2 nanotubes induces superior rate of matrix mineralization and osteofunctionality in human osteoblasts. Materials Science and Engineering: C. 2014; 37: 332–341. doi: 10.1016/j.msec.2014.01.014
17. Dong W, Cogbill A, Zhang T, et al. Multifunctional, catalytic nanowire membranes and the membrane-based 3D devices. The Journal of Physical Chemistry B. 2006; 110(34): 16819–16822. doi: 10.1021/jp0637633
18. Dong W, Zhang T, Epstein J, et al. Multifunctional nanowire bioscaffolds on titanium. Chemistry of Materials. 2007; 19(18): 4454–4459. doi: 10.1021/cm070845a
19. Xiao Y, Tian Y, Zhan Y, Zhu J. Degradation of organic pollutants in flocculated liquid digestate using photocatalytic titanate nanofibers: Mechanism and response surface optimization. Frontiers of Agricultural Science and Engineering. 2023; 10(3): 492–502. doi: 10.15302/J-FASE-2023503
20. Dong W, Zhang T, McDonald M, et al. Biocompatible nanofiber scaffolds on metal for controlled release and cell colonization. Nanomedicine: Nanotechnology, Biology and Medicine. 2006; 2(4): 248–252. doi: 10.1016/j.nano.2006.10.005
21. Shannon RD. Revised effective ionic radii and systematic studies of interatomic distances in halides and chalcogenides. Acta Crystallographica Section A. 1976; 32(5): 751–767. doi: 10.1107/S0567739476001551
22. Xue D, Luo J, Li Z, et al. Enhanced photoelectrochemical properties from Mo-doped TiO_2 nanotube arrays film. Coatings. 2020; 10(1): 75. doi: 10.3390/coatings10010075
23. Wang X, Liu SJ, Qi YM, et al. Behavior of potassium titanate whisker in simulated body fluid. Materials Letters. 2014; 135: 139–142. doi: 10.1016/j.matlet.2014.07.145
24. de Souza Balbinot G, da Cunha Bahlis EA, Visioli F, et al. Polybutylene-adipate-terephthalate and niobium-containing bioactive glasses composites: Development of barrier membranes with adjusted properties for guided bone regeneration. Materials Science and Engineering: C. 2021; 125: 112115. doi: 10.1016/j.msec.2021.112115

Appendix

XRD analysis of K-titanate NFs with various doping ratio.

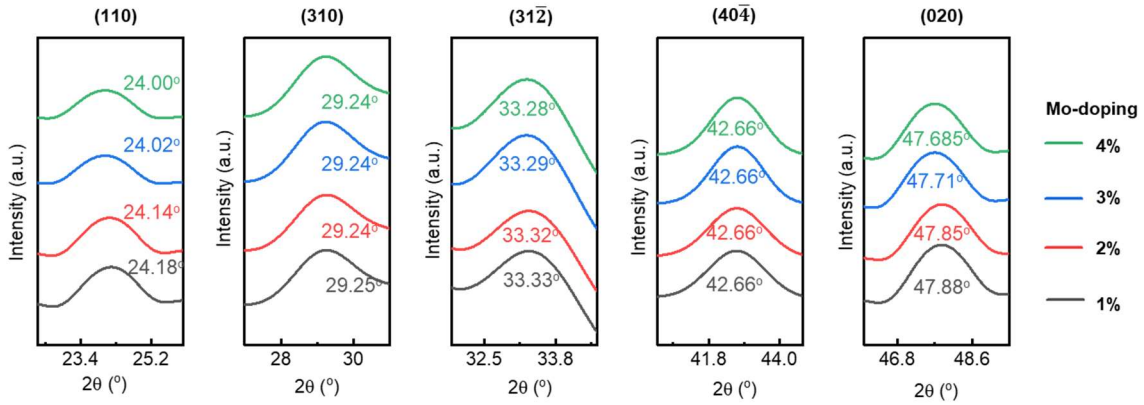

Figure A1. XRD peak shift analysis of K-titanate NFs with various doping ratio.